Heliyon 11 (2025) e42932

Contents lists available at ScienceDirect

Heliyon

journal homepage: www.cell.com/heliyon

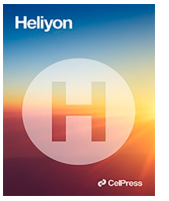

Research article

Adsorption kinetics and mechanisms of nano chitosan coated cotton fiber for the removal of heavy metals from industrial effluents

Md. Hasinur Rahman [a,b], Md. Marufuzzaman [a], Md. Aminur Rahman [a,c], Md. Ibrahim H. Mondal [a,*]

[a] Polymer and Textile Research Laboratory, Department of Applied Chemistry and Chemical Engineering, Rajshahi University, Rajshahi 6205, Bangladesh
[b] Jamuna Fertilizer Company Ltd., Bangladesh Chemical Industries Corporation (BCIC), Jamalpur-2055, Bangladesh
[c] Department of Public Health Engineering (DPHE), Zonal Laboratory, Khulna-9100, Bangladesh

ARTICLE INFO

Keywords:
Nanochitosan
Cotton fiber
Heavy metals
Adsorption
Citric acid
Kinetics

ABSTRACT

The present study successfully removed heavy metals from industrial effluent using nanochitosan-coated cotton fiber (NCCF) crosslinked with citric acid, demonstrating the potential of advanced technologies in removing heavy metals from large amounts of wastewater caused by the world's unchecked population growth and widespread industrialization that has caused pollution. Structural, morphological, and thermal properties of NCCF were determined. Results revealed that the nanochitosan component improves the adsorption capacity of cotton fiber (CF) through the increased surface area and porosity of NCCF. Sorption studies were conducted based on pH, kinetics, isotherms, and desorption results. The Langmuir and Freundlich adsorption isotherms were utilized to examine the CF and NCCF adsorption mechanisms. NCCF exhibited maximum Langmuir adsorption capacities of 4.76 mmol/g for Cd^{2+}, 6.40 mmol/g for Pb^{2+}, and 12.50 mmol/g for Cr^{6+}. Kinetic studies revealed that the pseudo-first-order kinetics model best describes the adsorption process. The results of the adsorption kinetics study showed that NCCF has a shorter half-time of adsorption than CF does during the adsorption process. This suggests that NCCF has a greater initial adsorption rate and adsorption capacity than CF. These findings are expected to lead to industrial applications in wastewater treatment as sustainable and highly effective materials.

1. Introduction

Rapid urbanization and industrialization have made water contamination a major worldwide problem in recent decades. Among the wide range of contaminants found in wastewater, heavy metals (HMs) are the most significant pollutants in effluents. Due to their toxicity, environmental durability, bioaccumulation, and biomagnification, these pollutants pose a serious threat to human health and have severely limited the availability of safe drinking water [1–3]. HMs that enter the food chain, including cadmium (Cd), chromium (Cr), mercury (Hg), copper (Cu), lead (Pb), manganese (Mn), nickel (Ni), zinc (Zn), and iron (Fe), are non-biodegradable and extremely

* Corresponding author.
E-mail address: mihmondal@gmail.com (Md.I.H. Mondal).

https://doi.org/10.1016/j.heliyon.2025.e42932
Received 10 October 2024; Received in revised form 21 February 2025; Accepted 21 February 2025
Available online 22 February 2025

toxic. Consequently, they can cause cancer and severe damage to the liver, kidneys, and bones [4–7].

Various techniques like chemical precipitation, oxidation, coagulation, flocculation, ion exchange, membrane filtration, reverse osmosis, and electrodialysis can remove HMs from wastewater [8,9]. However, these processes have drawbacks like high energy requirements, expensive costs, fouling, and the creation of hazardous byproducts, and the process endures for a long time [10–12]. Meanwhile, the adsorption process is widely recognized as the preferred approach for effectively eliminating HMs from wastewater [13]. This preference is due to its simple design, impressive efficiency, ease of use, minimal production of biological and chemical sludge, economic viability, reusability, potential for metal recovery, and wide availability [11,14]. Various natural and synthetic adsorbents for wastewater HMs ion removal have been devised recently: activated carbon, graphene, nanotubes, peat moss, biochar, films, hydrogels, and aerogels [8,9,15,16]. Along with silica, zeolites, sand bricks, and clays, nanoparticles, metal-organic frameworks, and magnetic materials have been used [10]. However, most of these materials are non-renewable or nonbiodegradable and may cause secondary pollution. They also have poorer efficiency, high energy and chemical reagent costs, capital outlays, and operational expenditures [17]. For this reason, a number of natural fiber-based materials have been investigated, including starch, sugar cane bagasse, chitosan, kapok, luffa fibers, lignocellulosic jute fiber, wheat straw, peanut and coconut shells, rice husks, and bamboo shoots [16,18].

Cotton-derived cellulose is one of the most versatile natural fibers and a very promising material for environmental detoxification among the numerous biopolymers. This is due to its softness, absorbency, renewability, low density, lightweight, low cost, and eco-friendliness [19–22]. Cotton, in its unaltered state, possesses surface functional groups (S=O, O-H, C=O, C–O, and C–H) that render it efficacious for the removal of HMs [23]. Despite possessing functional groups, cotton has a few drawbacks in its application as an adsorbent, including low adsorption capacity, microbial degradation, poor durability, shrinkage, and UV susceptibility [24,25]. To, firstly, improve cotton fiber's surface properties and interaction with pollutants in solution and secondly, its efficacy as a HMs adsorbent, various inorganic and organic materials have been used to incorporate specific functional groups for instance e.g., carboxyl, amino, ester, mercapto, cyclodextrin, and olefin [26–29].

Several researchers conducted studies on the impact of chitosan on cotton concerning the removal of HMs [17,22,30,31]. Chitosan, a natural polymer with desirable properties like hydrophilicity, biocompatibility, biodegradability, and non-toxicity, is ideal for modifying cotton and removing HMs from wastewater and can be enhanced by chemical alteration with cross-linking agents [30–32]. Although chitosan can remove HMs contaminants, there are still concerns over its availability issue is the limited durability and certain environmental toxicity risks in its bulk form [33].

Consequently, scientists have synthesized chitosan-based adsorbents that are more efficient. Rahaman et al. [22] synthesized a low-cost eco-friendly composite adsorbent using graphene oxide, carboxymethyl cellulose and chitosan for the adsorption of HMs from water. The substantial sorption values of Co^{2+}, Cr^{6+}, Mn^{2+} and Cd^{2+} were reported as 43.55, 77.70, 57.78 and 91.38 mg/g, respectively, under acidic conditions. In another research, acid-modified chitosan adsorbent was prepared by Rahaman et al. [22]. The maximum Langmuir adsorption capacities of Cr, Pb and Cd were reported to be 55, 80 and 91 mg/g, respectively, at pH 4 when the metal concentration and adsorbent dose were 120 mg/L and 1.0 g/L, respectively. Chitosan nanoparticles (CNPs) are highly effective nano-adsorbents because of their large surface area, exceptional adsorption ability, and eco-friendly nature (Rahaman et al., 2021; add another 2 references). Ali et al. [34] employed chitosan nanoparticles (NPs) to eliminate Fe(II) and Mn(II) via adsorption, achieving a capacity of 116.2 mg/g and 74.1 mg/g, respectively. Abd Elhakeem et al. [35]. Documented that the adsorption of nano chitosan for Fe (II) and Mn(II) achieved a remarkable efficiency of 99.94 % and 80.85 %, respectively. Liu et al. [36] conducted a study where magnetic CNPs were employed to remove As(V) and As(III). The results demonstrated a high removal capacity of 95 % (≈144.75 mg/g) for both As(V) and As(III) within a short duration of 15 min. The dominant mechanism, in this case, is the electrostatic attraction between the positive surface charges of the protonated chitosan amine functions and the negative charges of the arsenate ions. Seyedi et al. [37] employed magnetic CNPs to remove Cd(II), and they applied the Langmuir adsorption isotherm. While CNPs have proven to be successful in eliminating HMs from polluted water, there are lingering questions regarding their accessibility, durability, and ability to adsorb various metal ions from wastewater.

For this reason, it is imperative to enhance the development of materials that exhibit enhanced stability and possess the ability to effectively eliminate numerous pollutants in complex environments. Furthermore, it is necessary to develop cost-effective, high-performing, and reusable adsorbents for their practical utilization. To accomplish this goal, chitosan was obtained from discarded shrimp shells and produced nano chitosan by combining it with sodium tripolyphosphate (STPP) in a solution of acetic acid. In response to the aforementioned constraints of cotton and chitosan in the context of HM decontamination, a composite of these two substances has been developed to enhance efficacy. We have attempted to examine the specified composition, which is cross-linked with citric acid, for the effective removal of several toxic ions such as Cr^{6+}, Cd^{2+}, and Pb^{2+} from wastewater. This study also aimed to ascertain the adsorption processes and kinetics of both untreated cotton (CF) and cotton fiber coated with nanochitosan (NCCF), as well as their capacity for adsorption at equilibrium.

2. Materials and methods

2.1. Materials

100 % cotton fiber was collected from a textile factory, located in Rajshahi, Bangladesh. Sodium hydroxide, acetic acid, citric acid, absolute alcohol, hydrochloric acid and potassium dichromate were sourced from Merck (Germany). Sodium tri-polyphosphate (STPP) was purchased from Merck (India and Germany). Surfactant Tween 80, Nickel Chloride was bought from Sigma Aldrich (USA). All chemicals used in this research were of analytical grade with purities of ≥99 %. The purity of these chemicals ensured the reliability

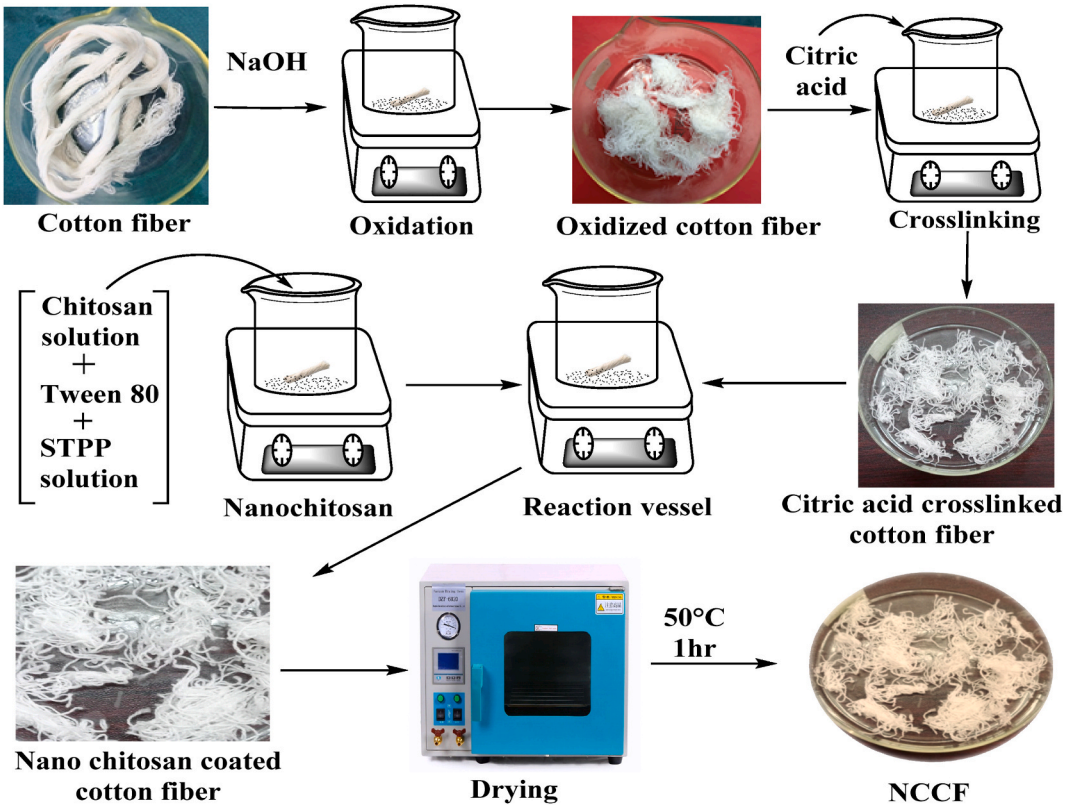

Fig. 1. Preparation of nanochitosan and NCCF.

and reproducibility of the experimental results. Detailed specifications and certificates of analysis for each chemical were provided by the respective suppliers and are available upon request. Deionized (DI) water was used for all solution preparation throughout the experiment.

2.2. Preparation of chitosan nanoparticles

Chitosan was extracted from waste prawn shells by demineralization and deprotenization. Then the ionic gelation method was employed to prepare CNPs by inducing the gelation of a CS solution with sodium tripolyphosphate (STPP). For this purpose, a chitosan solution of 0.1 % was prepared by dissolving 200 mg of chitosan in 200 mL of 1 % acetic acid solution. The pH of the solution was adjusted to 4 by adding 0.1 N NaOH dropwise, followed by adding 5 % Tween 80 to the chitosan solution to prevent particle aggregation. Secondly, an STPP solution of 0.1 % was prepared by dissolving 10 mg of STPP in 10 mL of deionized water. The solution was filtered using Whatman filter paper, grade 42. Finally, STPP solution was added dropwise with a syringe to chitosan solution under magnetic stirring conditions at 800 rpm at room temperature in the ratio 2.5: 1 (v/v) (chitosan: STPP). The resulting chitosan particle suspension was centrifuged at 900 rpm for 30 min. The nano chitosan obtained was in the form of a dispersed solid. The CNPs suspension was then freeze-dried before further analysis was undertaken [38,39].

2.3. Modification of cotton with nanochitosan

Cotton fibers (CFs) were manually cleaned with detergents to remove impurities, boiled in water for 2 h, and submerged in 0.1M NaOH for 1 h at 25 °C. Then it was rinsed with deionized water until a constant pH was obtained. After washing, the fibers were dried in an oven at 50 °C for 2 h [40]. The CFs were placed in solutions of 0.97 M citric acid with a liquor ratio of 1:50. After shaking at 100 rpm for 1 h at 90 °C, fibers were rinsed with deionized water until the pH of the rinse water remained constant and then it was oven-dried at 90 °C for 1 h [41]. The modified cotton fiber was exposed to the CNPs suspension and magnetically stirred at 300 rpm for 24 h at room temperature. Following that, the nanochitosan coated cotton fibre (NCCF) was filtered, and subsequently allowed to air dry for 24 h at 25 °C. Fig. 1 illustrates the preparation process of nanochitosan and nanochitosan coated cotton fiber [42].

2.4. Fiber characterization

Infrared spectra (IR) were recorded on a Fourier transform infrared (FTIR) spectrophotometer (Model: FTIR- 1000, PerkinElmer

(UATR two), USA). For this purpose, the sample was cut into small pieces and approximately 0.1 g–1 g of the fiber pieces were placed on the ATR plate. Afterwards, the IR spectra of the sample were recorded in the 4000 to 400 cm^{-1} range. The morphology of the samples was characterized using a scanning electron microscope (SEM) (FEI Quanta Inspect, Model: S50, Netherlands). The samples were magnified 5100 times and scanned at 5 kV. The thermal stability and the degradation rate of the modified and unmodified samples were recorded using a thermogravimetric analyzer (TGA) and differential thermal analyzer (DTA) (SEIKO- EXTAR TG/DTA-6300, Japan). About 50.0 mg of the sample was crushed in an agate mortar. Then the samples were analyzed for TG analysis in the temperature range of 30–700 °C under the heating rate of 10 °C/min. The pressure was constantly maintained at 101 kPa. The concentration of metal ions in 25 mL aqueous solution was determined using a 932 B-model atomic adsorption spectrometer (AAS), GBC, Australia.

2.5. Analysis of moisture content

A moisture analyzer machine serves to determine the moisture content of CF and NCCF. The "Loss On Drying Method" was utilized to ascertain moisture loss by subtracting the weight of dried samples (at 120 °C) from that of one carrying moisture [43].

2.6. Adsorption isotherm

The primary method deployed to conduct adsorption isotherm experiments was to determine the adsorbent's adsorption capacity and equilibrium adsorbent concentration in the solution [44,45]. For this reason, five different amounts of adsorbent were added to a conical flask containing 10 mL of the known concentration solutions of heavy metals at 298 K, and the pH of the solution was in the 6–7 range. Then the samples were starved for 24 h with the help of a flask shaker. After 24 h, the equilibrium concentrations of the adsorbent were determined with the help of a UV–Vis spectrophotometer. The adsorption capacity and removal percentage (%) of HMs onto NCCF [13] were calculated by the following equations (1) and (2).

$$q_e = [(C_0 - C_e) \times V] / W \quad (1)$$

$$\% \text{ Removal} = [(C_0 - C_e) \times 100] / C_0 \quad (2)$$

Where q_e (mg/g) represents the adsorbed amount of HMs by the adsorbent, C_0 and C_e are the initial and equilibrium HMs concentration (mg/L), respectively while V is the total volume (L) of the reaction medium and W is the weight (g) of adsorbent.

Also, two isotherm models were utilized to determine the effective adsorption process.

The Langmuir isotherm can be expressed by equation (3):

$$\frac{1}{q_e} = \frac{1}{q_m} + \frac{1}{q_m K_L} \frac{1}{Ce} \quad (3)$$

Where q_m denotes the maximal monolayer adsorption capacity (mg/g), K_L stands for the Langmuir isothermal constants (L/mg), q_e is the equilibrium adsorption capacity (mg/g) and C_e represents the equilibrium concentration of a heavy metal ion in the solution (mg/L) [46,47].

Furthermore, the study of the CF and NCCF adsorbents used the Freundlich adsorption isotherm constants using equation (4):

$$\log q_e = \log k_f + \frac{1}{n} \log C_e \quad (4)$$

where, q_e is the adsorption capacity, C_e stands for the equilibrium concentration of metal ions in solution (mg/L), n is the adsorption intensity, and k_f is the Freundlich constant with multilayer adsorption which is related to bond strength [48].

2.7. Adsorption kinetics

The batch kinetics experiments were executed in a way similar to the adsorption isotherm. Here, the adsorption was analyzed in terms of pseudo-first-order (PFO) reaction kinetics and second-order reaction (PSO) kinetics to determine the adsorption reaction kinetics parameter [49–51].

2.8. Adsorption thermodynamics

The feasibility of an adsorption reaction is determined by the thermodynamics of adsorption. The efficacy of a reaction is dependent on the negative change in free energy. The Langmuir adsorption constant, K_L (L/mg), was employed to calculate the free energy change (ΔG) of adsorption using the following equation (5):

$$\Delta G = -RT\ln k_c \quad (5)$$

where R is molar gas constant (8.314 $JK^{-1}mol^{-1}$), T is the absolute temperature (298 K) and k_c is the equilibrium constant [49,52]. The value of equilibrium constant can be determined by using following equation (6),

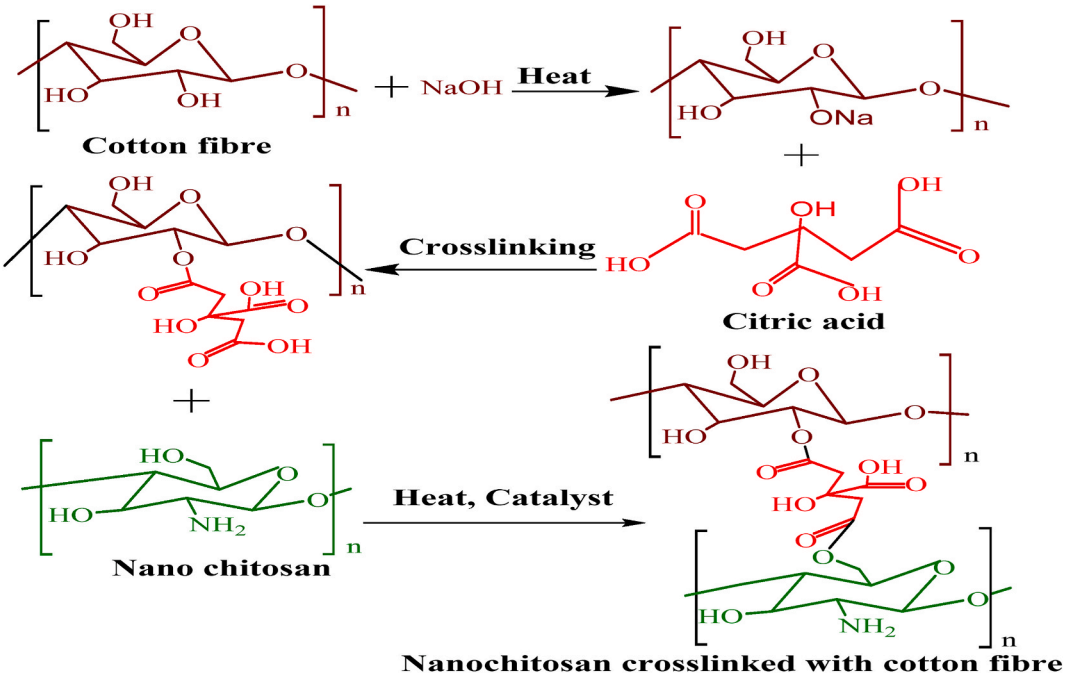

Fig. 2. Synthesis route of NCCF.

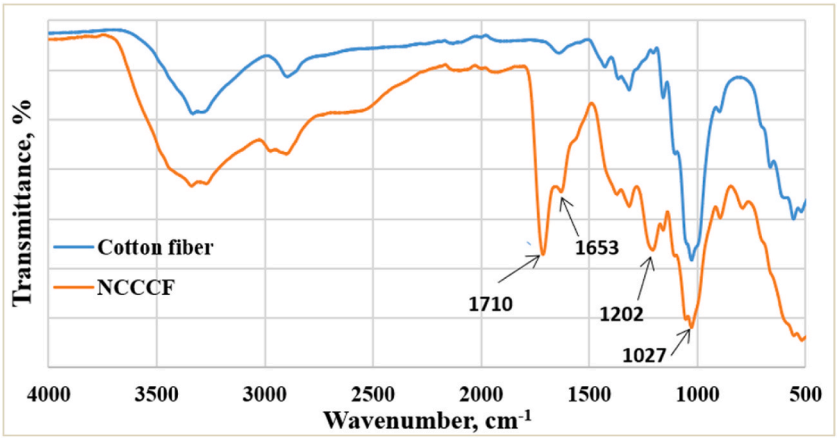

Fig. 3. Ftir spectra of RC and NCCF.

$$K_c = K_L \times M_w \times 55.5 \times 1000 \quad (7)$$

where M_W is the molecular weight of adsorbate molecule [53].

3. Results and discussion

3.1. Modification mechanism

In an acidic environment, nanochitosan is chemically bonded to cotton fiber (CF) using citric acid. The procedure entails the treatment of the cotton fiber with sodium hydroxide, which is followed by the removal of a water molecule, resulting in the attachment of citric acid. Lastly, the citric acid establishes an ester linkage between the cotton fiber and nanochitosan, thereby serving as a bridge [46,54]. Fig. 2 schematically illustrates the reaction mechanism.

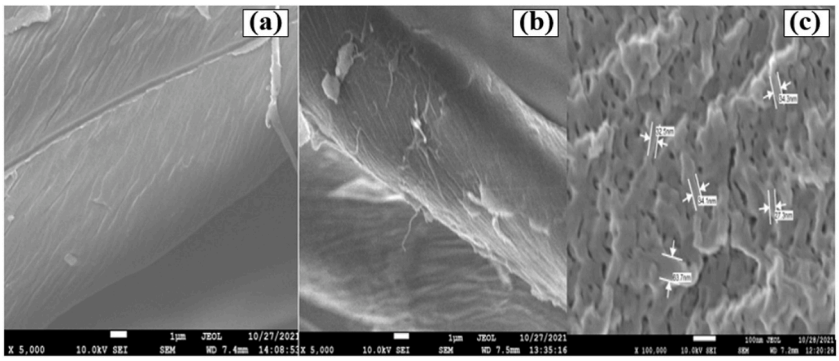

Fig. 4. SEM image of (a) RC; (b & c) NCCF.

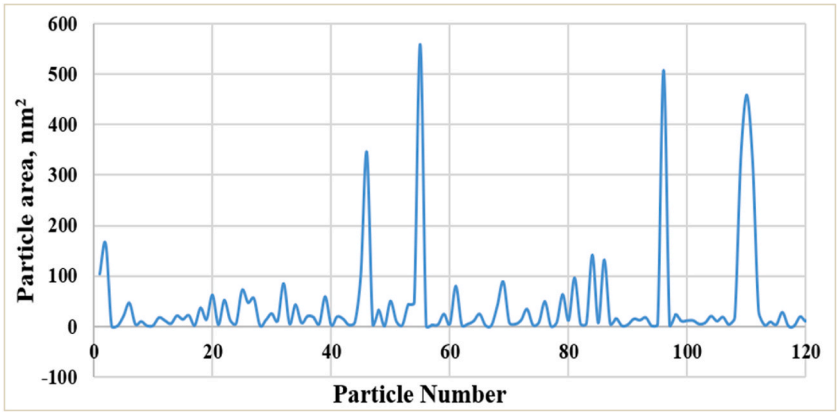

Fig. 5. Particle size distributions of nanochitosan particle with 'image J' software.

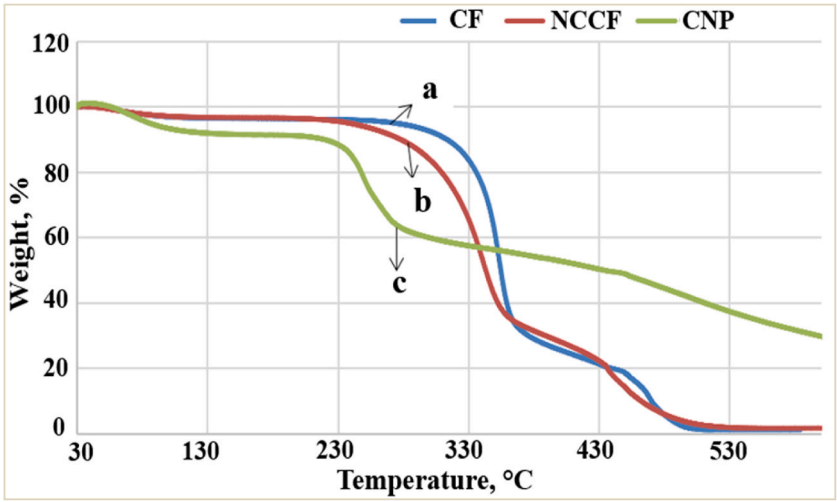

Fig. 6. TGA graph of (a) CF, (b) NCCF, and (c) CNP.

3.2. Fourier-transform infrared spectroscopy analysis

The FTIR analysis, as illustrated in Fig. 3, confirms the chemical attachment of nano chitosan to cotton fiber. The FTIR spectra of NCCF reveal the presence of the ester stretching band at 1710 cm^{-1}, which suggests that chitosan was covalently attached to cellulose through the formation of ester bonds [40,55]. The presence of C-O following the esterification reaction is indicated by the absorption

Table 1
Langmuir and Freundlich adsorption isotherm constants, and specific surface area (SSA) for CF and NCCF adsorbent.

Langmuir adsorption Constants of CF					Freundlich constants of CF		
Heavy metals	q_m (mg/g)	K_L (L/mg)	R_L	R^2	n	K_f (L/mg))$^{1/n}$	R^2
Cr^{6+}	7.12	0.0043	0.823	0.008	1.198	0.048	0.008
Pb^{2+}	6.08	0.022	0.479	0.020	1.51	0.237	0.037
Cd^{2+}	5.34	0.0083	0.708	0.004	0.567	0.002	0.018
Langmuir adsorption Constants of NCCF					**Freundlich constants of NCCF**		
Cr^{6+}	23.15	0.0225	0.470	0.323	1.40	0.804	0.191
Pb^{2+}	11.86	0.0115	0.634	0.829	1.40	0.266	0.232
Cd^{2+}	10.60	0.0226	0.468	0.695	1.84	0.677	0.116
SSA of CF (m^2/g) 39.88 ×10^6				SSA of NCCF(m^2/g) 84.70 ×10^6			

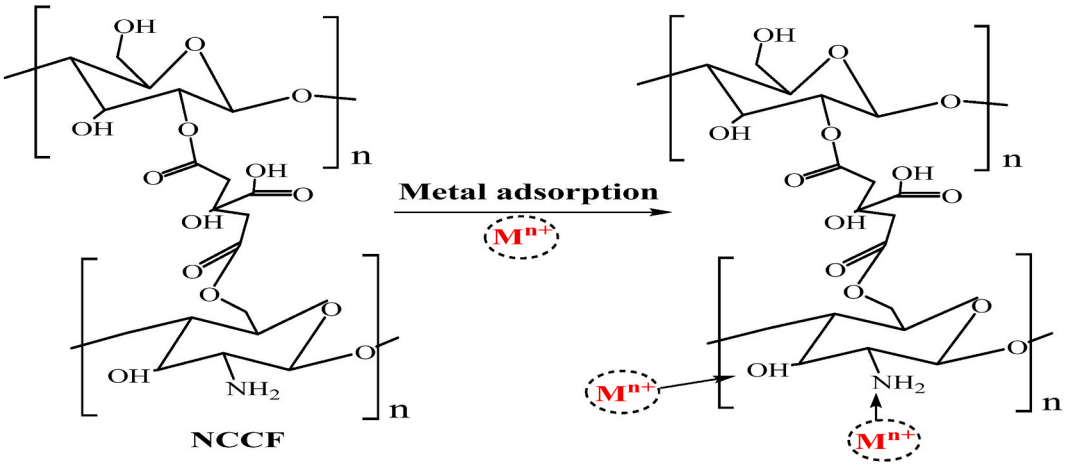

Fig. 7. Heavy metals adsorption mechanism of NCCF.

band at 1202 cm^{-1}. The FTIR spectra of the treated fibers also exhibit the absorption band at 1653 cm^{-1}, which is an outcome of the C=O stretching of the secondary amide of chitosan [56]. In addition, the absorption at a wavenumber of 1027 cm^{-1} confirmed the presence of the C-O-C (polysaccharide) functional group in NCCF [57,58].

3.3. Scanning electron microscopy analysis

The SEM micrographs of cotton fiber (CF) and NCCF are shown in Fig. 4. It can be observed that the surface of cotton fiber (Fig. 4a) was smoother than that of NCCF (Fig. 4b). As well, the surface of NCCF became rough with some different-depth longitudinal stripes generation and also showed a veil-forming effect on the cellulose fibers (Fig. 4c), indicating that the nano chitosan was effectively attached to the cotton fibre [40,59].

3.4. Particle size analysis by 'image J' software with SEM image

Nanoparticles can be differentiated from SEM images of nano chitosan by employing 'imageJ' software, which generates particle size analysis graphs that display the average number and area dimension (nm^2) [60]. The sharp peaks as illustrated in Fig. 5 indicate nano chitosan particles on cotton fiber surfaces are in the nano range (particle diameter <100 nm), as validated by SEM analysis in Fig. 4.

3.5. Thermal analysis

Fig. 6 illustrates the TGA thermograms, which exhibit a weight loss peak for the nano chitosan, CF, and NCCF samples within the temperature range of 30 °C–600 °C. The nano chitosan experienced its first stage of deterioration between temperatures of 30–110 °C, resulting in an 8 % reduction in weight due to the loss of absorbed and bound water. The slight decrease in weight observed between 140 and 200 °C can be attributed to the degradation of polymers with low molecular weights, such as NH_3 and CO. A substantial weight reduction occurred between 243 and 360 °C, which can be attributed to a complex mechanism involving the removal of water from the anhydroglucosidic ring. Regarding cotton fiber, a significant decrease in weight occurs between temperatures of 243 °C and 360 °C,

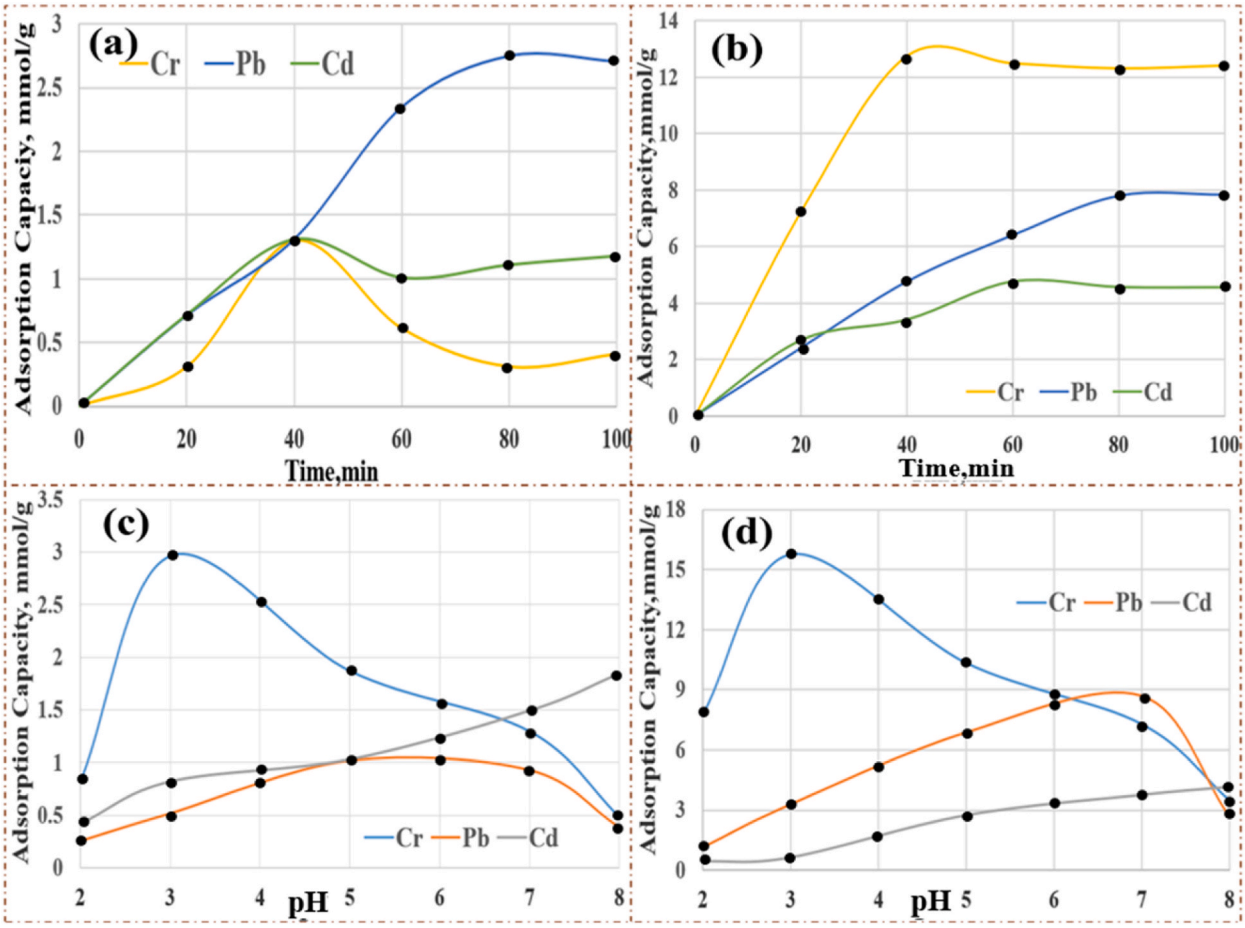

Fig. 8. Adsorption capacity of heavy metals for (a) CF with time, (b) NCCF with time, (c) CF with pH, and (d) NCCF with pH.

which signifies the breakdown of hemicelluloses and alpha celluloses [61,62]. However, when nanochitosan is bonded to the cotton fiber, the peak in the DTG graph within this temperature range suggests that the thermal stability declines slightly, providing further evidence of the nanochitosan coating on the cotton fiber as seen in FTIR and SEM analysis.

3.6. Moisture content of CF and NCCF

NCCF has a higher moisture absorption capacity than cotton fiber (CF). Since chitosan is hydrophilic, the moisture content of NCCF rises from 8 % to 12 %. With an increase in moisture content, chitosan has a propensity to undergo swelling. The expansion of chitosan may increase in its porosity and available surface area, which may have an indirect impact on its adsorption capacity [63].

3.7. Adsorption studies

3.7.1. Adsorption isotherm for CF and NCCF adsorbent

The adsorption of heavy metals (Cr^{6+}, Cd^{2+}, and Pb^{2+}) by CF and NCCF was investigated using Freundlich and Langmuir isotherms. According to the Langmuir isotherms, the maximum adsorption capacities were 4.76 mmol/g for Cd^{2+}, 6.40 mmol/g for Pb^{2+}, and 12.50 mmol/g for Cr^{6+} (Table 1 & Fig. 8). This may be attributed to the electronegativity of the metal, the hydration radius, the atomic weight of the metal and so on [17]. The mechanism by which NCCF adsorbs heavy metals is schematically illustrated in Fig. 7. The NCCF is affixed to heavy metal ions through the formation of bonds with OH and -NH_2 groups [54].

In Table 1, the separation factor (R_L) value for CF and NCCF in the adsorption of Cr^{6+}, Pb^{2+}, and Cd^{2+} is ranged from 0 to 1. This implies that monolayer adsorption is advantageous in all adsorption experiments [64]. Additionally, Table 1 indicates that the value of n for the NCCF adsorbent is greater than unity. This implies that the adsorption of metal ions by NCCF is proceeding favorably [65].

3.7.2. Effect of contact time

Fig. 8a and b illustrates the impact of contact time on the equilibrium adsorption of CF and NCCF. In this study, 30 mg of CF and

Table 2
A comparative analysis of the maximal adsorption capacities of Cr^{6+}, Cd^{2+}, and Pb^{2+} ions by various adsorbents.

Adsorbent	Adsorption capacity (mmol/g)			References
	Cr (VI)	Cd (II)	Pb (II)	
Zirconium- metal-organic frameworks (MOFs) (UiO-66-NH_2)/Polyacrylonitrile (PAN)/chitosan nanofibers composite (PAN/CTS/UiO-66-NH_2 MOF)	7.17	3.69	2.12	[67]
Glutaraldehyde cross-linked chitosan @ acid-activated bentonite composite (CsG@AAB)	5.46	–	2.18	[68]
Fe_3O_4/Covalent organic frameworks (COFs)-Polypyrrole magnetic composites (Fe_3O_4@COF-MT@PPy)	8.25	–	–	[69]
Hydroxyapatite (Hap)	–	0.95	7.71	[70]
Chlorapatite (Clap)	–	0.70	7.13	[70]
Fluorapatite (Fap)	–	0.14	7.03	[70]
Abiotic adsorbent Ca^{2+}- metal-organic frameworks (Ca-MOF)	–	1.96	2.51	[71]
Fe_3O_4/chitosan/3-Aminopropyltrimethoxysilane composite (Fe_3O_4@CS-APTMS)	5.18	–	–	[72]
Aminopropyltriethoxysilane (APS) modified microfibrillated cellulose (MFC)	–	4.19	–	[73]
Glycidyl methacrylate Functionalization of cellulose	9.6	–	–	[74]
Sodium bicarbonate treated sodic cellulose nanocrystals (NaSCNCs)	–	3.06	2.24	[75]
poly (acrylic acid) grafted chitosan and biochar composite (PAA/CTS/BC)	–	3.29	2.29	[76]
carboxyl methylcellulose/chitosan/poly (dopamine)/Polyethyleneimine bead CMC/CS/PDA@PEI	–	4.18	6.67	[77]
Graphene oxide/CT aerogel microspheres	5.6	–	2.12	[78]
Chitisan and lysozyme biocomposite	4.1	–	3.6	[79]
Waste cotton fabrics-based polyacrylamide double network hydrogel (WCF/PAM DNH)		1.76	1.84	[80]
Polydopamine-modified-Chitosan aerogels	7.2	–	–	[81]
Magnetic biochar	–	–	3.95	[82]
Chitosan/Titanium dioxide	1.77	–	2.29	[83]
aminopropyltriethoxysilane-functionalized biochar grafted on MXene (APTES/BC/MXene composite)			2.16–5.17	[84]
Nanochitosan coated cotton fiber (NCCF)	12.50	4.76	6.40	[Present study]

NCCF was added to each adsorbent solution, which was then treated for varying amounts of time (20, 40, 60, 80, and 100 min) [66]. Both the temperature and pH were maintained at 25 °C and 4.

Fig. 8a demonstrates that the adsorption of Cr exhibits a declining trend, as opposed to a plateau trend, as illustrated by the blue curve (Pb). The yellow curve's decline is more pronounced than that of the green curve (Cd). Therefore, the cotton fiber that has not been modified is unsuitable for Cr adsorption after 40 min. Consequently, the cotton fiber must be modified, as evidenced by the results in Fig. 8b. However, time-dependent increases in adsorption capacities were observed for both CF and NCCF, with the highest adsorption capacity occurring between 40 and 60 min of contact time due to the increased adsorption reaction mechanism of both CF and NCCF. NCCF has the following equilibrium adsorption capacities: Cr^{6+} (12.50 mmol/g), Pb^{2+} (6.40 mmol/g), Cd^{2+} (4.76 mmol/g). A comparative analysis of the maximal adsorption capacities of the heavy metal ions from effluent by various adsorbents, as illustrated in Table 2, indicates that NCCF is a viable alternative for the adsorption of Cr^{6+}, Pb^{2+}, and Cd^{2+} ions from wastewater.

3.7.3. Effect of pH on heavy metals adsorption capacity

pH is an important parameter for the adsorption of NCCF. At a low pH environment (pH < 7), amine groups in NCCF could be easily protonated, which induced an electrostatic force, therefore, the adsorption capacity of NCCF is higher, while it is lower in the basic pH range, as a result of the increased availability of surface charge. At low pH, the cationic sites (NH_3^+) of functional groups are considered to be more significant than the anionic sites (OH-) during the adsorption process due to their capacity to chelate with metal ions. Heavy metal ions precipitate in basic media with a pH greater than 8 due to the diminished availability of surface charge [85,86] (Fig. 8c and d).

3.7.4. Adsorption kinetics

The SSA of NCCF is approximately doubled when coated with nan ochitosan, as shown in Table 1. Nanochitosan coating on CF substantially doubles its SSA from 39.88×10^6 m^2/g to 84.7×10^6 m^2/g. The value of n is greater than unity ($1 < n < 10$), which means favorable adsorption of NCCF. Table 1 indicates that the initial adsorption rate of NCCF is greater than that of CF, with a value of U mg/g. min. The half-time adsorption of NCCF is less than that of the cotton fiber (CF), suggesting that the adsorption time for NCCF is short. Additionally, the maximal adsorption capacity of NCCF surpasses that of CF. The adsorption kinetic models (PFO & PSO) have been used to evaluate the performance of the adsorbent and to investigate the adsorption mass transfer mechanisms. From Fig. 9(a–f) & Fig. 10(a–f), for the range of values of R^2, some generalizations can be made. For example, values of $R^2 < 0.5$ indicate a weak relation between the predictor (or independent) variable(s) and the response variable, while $0.5 < R^2 < 0.8$ indicate that the model is not adequate and $R^2 \geq 0.8$ indicate a good fit between the data and the model [87]. As demonstrated in Fig. 10a-f, the pseudo-second-order (PSO) model exhibited low R^2 values. Because of the greater correlation discrepancy from unity, the data did not align with the PSO kinetic model. These findings demonstrated that the pseudo-second-order model did not adequately correspond to the experimental data. For this reason, the adsorption of heavy metals onto NCCF was not a pseudo-second-order reaction. The pseudo-first-order (PFO) model, in contrast, generated R^2 values that were virtually identical to unity, as illustrated in Fig. 9a-f. The PFO model was found to be appropriate for characterizing the adsorption process of Cr^{6+}, Cd^{2+}, and Pb^{2+} onto NCCF, as the results indicated.

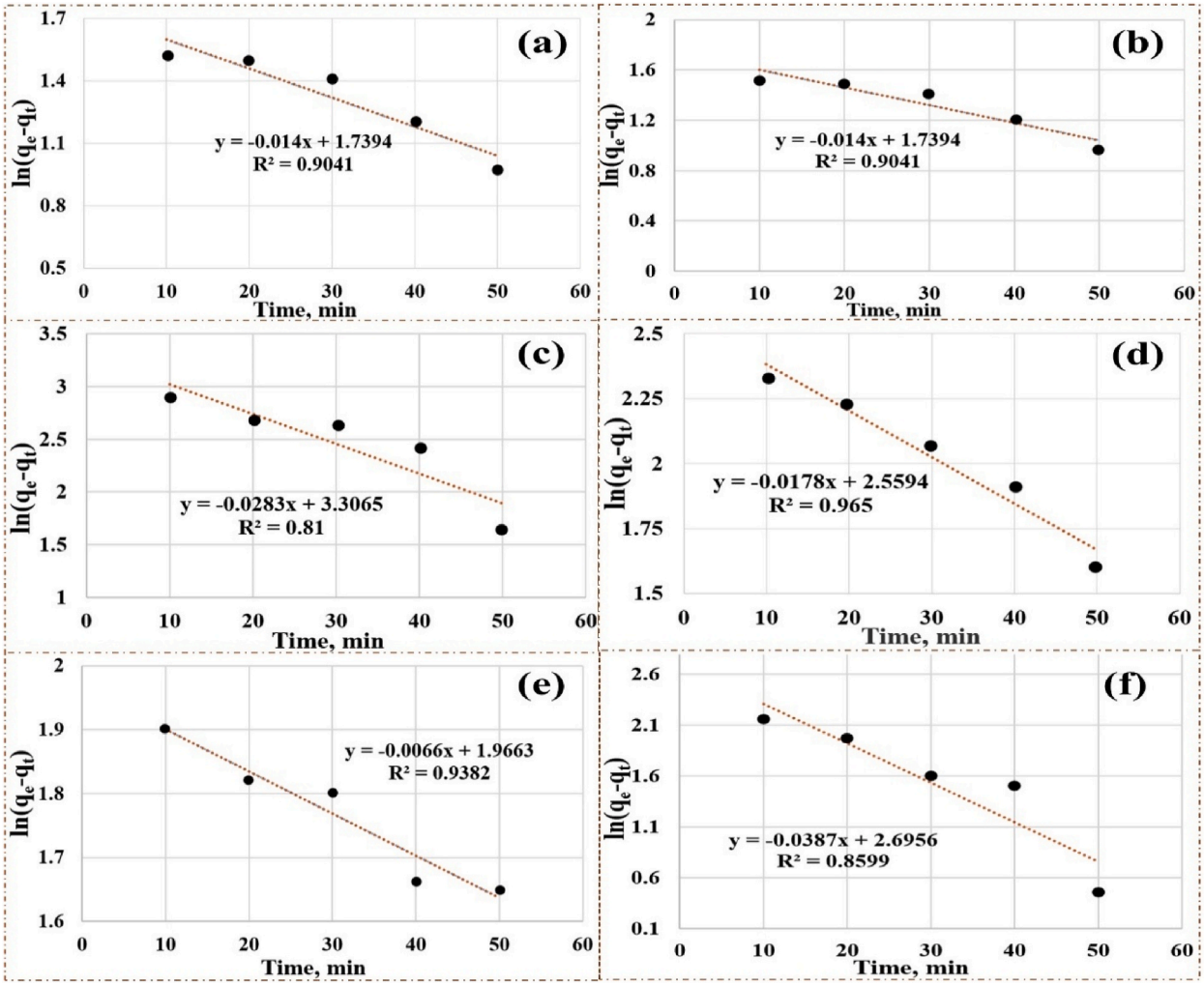

Fig. 9. PFO kinetics modelling of (a) Cr^{6+}, (b) Cd^{2+}, and (c) Pb^{2+} for CF, and (d) Cr^{6+}, (e) Cd^{2+}, and (f) Pb^{2+} for NCCF.

Hence, during the adsorption of heavy metals by NCCF the rate-limiting step is the adsorption onto active sites. In this sense, the external diffusion or the internal diffusion is the rate-controlling step. Additionally, the adsorption rate is determined by the particle diffusion mechanism, as evidenced by Table 1 & Fig. 9. It is important to note that the adsorption rates for Cr^{6+}, Cd^{2+}, and Pb^{2+} were significantly delayed for NCCF, as indicated by the adsorption kinetics above. This could be the consequence of the faster interaction rate of Cr^{6+}, Cd^{2+}, and Pb^{2+} with coordination atoms [86]. Consequently, a metal complex matrix was swiftly formed around the chitosan particle, which impeded the diffusion of the metal into the interior of the NCCF particle.

3.7.5. Adsorption thermodynamics

For significant adsorption to occur, the Gibb's free energy change of adsorption, ΔG^0, must be negative. The thermodynamic parameters of the adsorption of Cr^{6+}, Cd^{2+}, and Pb^{2+} onto NCCF were calculated and presented in Table 3. Negative values of ΔG^0 are obtained as a consequence of the adsorption of Cr^{6+}, Cd^{2+}, and Pb^{2+} by NCCF. This confirms that the heavy metals adsorption process onto NCCF was spontaneous. This implies that the adsorptions of heavy metals on NCCF was thermodynamically feasible and spontaneous at room temperature [49,52,88].

4. Conclusion

This study prepared NCCF from cotton fiber and nanochitosan by ester bond creation cross-linked by citric acid, the objective being to remove Cr^{6+}, Cd^{2+}, and Pb^{2+} from effluent. The best NCCF adsorption capabilities were 4.76 mmol/g Cd^{2+}, 6.40 mmol/g Pb^{2+}, and 12.50 mmol/g Cr^{6+}. The CF and NCCF adsorption mechanisms were studied using Langmuir and Freundlich isotherms. Nanochitosan coating on CF substantially doubles its SSA from 39.88×10^6 m^2/g to 84.7×10^6 m^2/g. NCCF's SSA thus boosts heavy metal adsorption to an acceptable level. NCCF had a shorter half-time of adsorption than CF in the adsorption kinetics research. Shown here is that NCCF

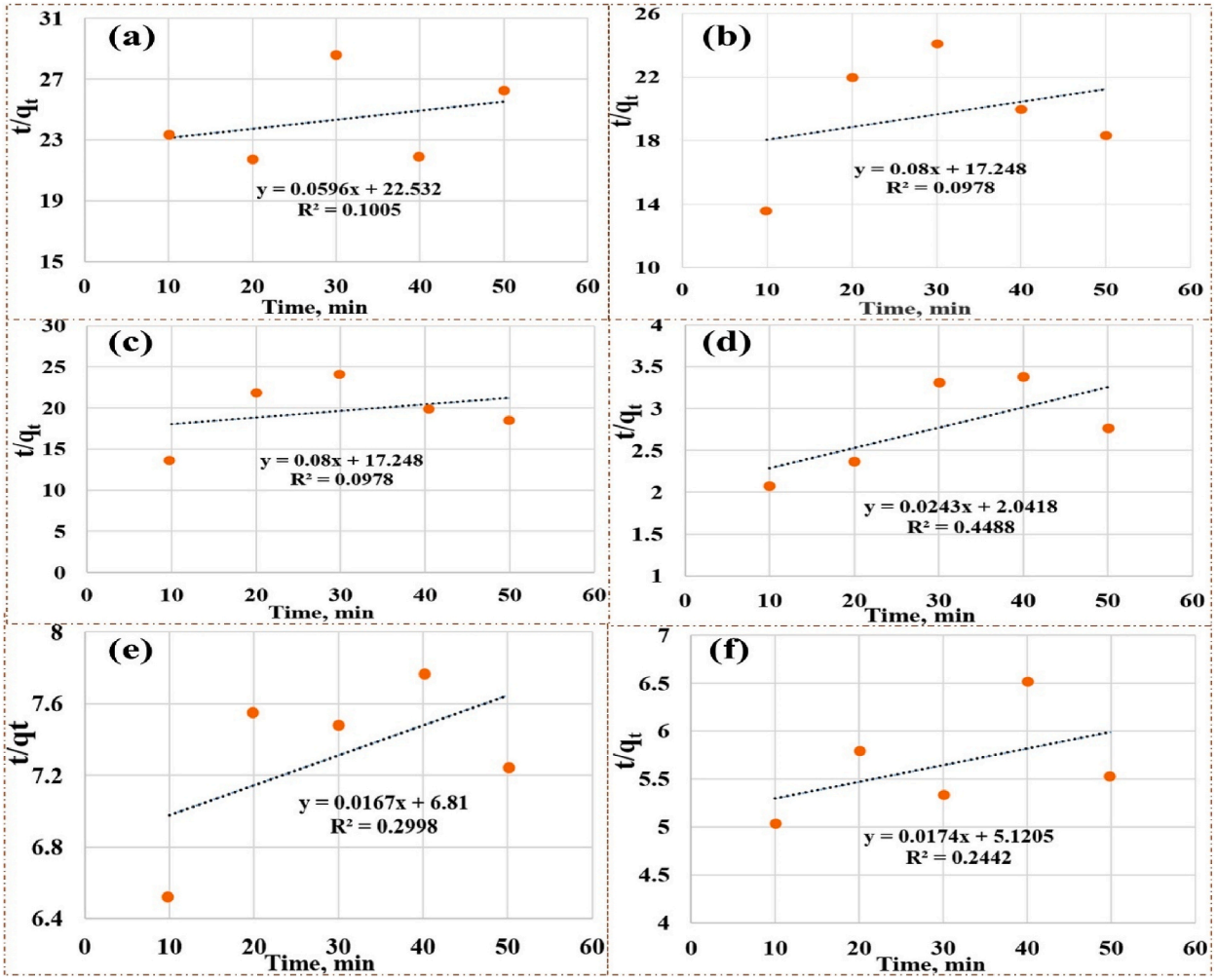

Fig. 10. PSO kinetics modelling of (a) Cr^{6+}, (b) Cd^{2+}, and (c) Pb^{2+} for CF, and (d) Cr^{6+}, (e) Cd^{2+}, and (f) Pb^{2+} for NCCF.

Table 3
Determination of ΔG^0 for heavy metals (Cr^{6+}, Cd^{2+}, and Pb^{2+}) adsorption.

Name of the heavy metal ions	Adsorbent	Langmuir Constant, K_L, L/mg	Equilibrium constant, k_c	ΔG^0 (KJ/mol)
Cr^{6+}	CF	0.0043	12.4×10^3	−23.35
	NCCF	0.0353	101.8×10^3	−28.56
Pb^{2+}	CF	0.022	252.9×10^3	−30.82
	NCCF	0.0115	132.2×10^3	−29.22
Cd^{2+}	CF	0.0083	51.7×10^3	−26.88
	NCCF	0.0226	140.9×10^3	−29.37

has a higher initial adsorption rate and capacity than CF. Thus, we expect that this type of surface alteration can improve cotton fabric's sustainability and usability, encouraging its wide variety of wastewater treatment applications. However, further research into the NCCF's mechanical and antibacterial properties is required as it could lead to an affordable fabric water filter.

CRediT authorship contribution statement

Md. Hasinur Rahman: Writing – original draft, Visualization, Methodology, Investigation, Formal analysis. **Md. Marufuzzaman:** Writing – original draft, Visualization, Methodology, Investigation, Formal analysis. **Md. Aminur Rahman:** Writing – original draft, Visualization, Methodology, Formal analysis. **Md. Ibrahim H. Mondal:** Writing – review & editing, Supervision, Resources, Funding acquisition, Formal analysis, Conceptualization.

Data availability

Data will be made available on request.

Declaration of competing interest

The authors declare that they have no known competing financial interests or personal relationships that could have appeared to influence the work reported in this paper.

References

[1] H.S. Budi, M.J.C. Opulencia, A. Afra, W.K. Abdelbasset, D. Abdullaev, A. Majdi, M. Taherian, H.A. Ekrami, M.J. Mohammadi, Source, toxicity and carcinogenic health risk assessment of heavy metals, Rev. Environ. Health 39 (1) (2024) 77–90, https://doi.org/10.1515/reveh-2022-0096.

[2] M. Taghavi, A. Shadboorestan, L.R. Kalankesh, A. Mohammadi-Bardbori, H.R. Ghaffari, O. Safa, G. Farshidfar, M. Omidi, Health risk assessment of heavy metal toxicity in the aquatic environment of the Persian Gulf, Mar. Pollut. Bull. 202 (2024) 116360, https://doi.org/10.1016/j.marpolbul.2024.116360.

[3] G.I. Edo, P.O. Samuel, G.O. Oloni, G.O. Ezekiel, V.O. Ikpekoro, P. Obasohan, J. Ongulu, C.F. Otunuya, A.R. Opiti, R.S. Ajkaye, A.E.A. Essaghah, J.J. Agbo, Environmental persistence, bioaccumulation, and ecotoxicology of heavy metals, Chem. Ecol. 40 (3) (2024) 322–349, https://doi.org/10.1080/02757540.2024.2306839.

[4] P.B. Angon, M.S. Islam, S. Kc, A. Das, N. Anjum, A. Poudel, S.A. Suchi, Sources, effects and present perspectives of heavy metals contamination: soil, plants and human food chain, Heliyon 10 (7) (2024) e28357, https://doi.org/10.1016/j.heliyon.2024.e28357.

[5] N. Verma, M. Rachamalla, P.S. Kumar, K. Dua, Assessment and impact of metal toxicity on wildlife and human health, in: S.K. Shukla, S. Madhab (Eds.), Metals in Water, Elsevier, 2023, pp. 93–110, https://doi.org/10.1016/B978-0-323-95919-3.00002-1.

[6] A. Sharma, A.S. Grewal, D. Sharma, A.L. Srivastav, Heavy metal contamination in water: consequences on human health and environment, in: S.K. Shukla, S. Madhab (Eds.), Metals in Water, Elsevier, 2023, pp. 39–52, https://doi.org/10.1016/B978-0-323-95919-3.00015-X.

[7] S.C. Chakraborty, M. Qamruzzaman, M.W.U. Zaman, M.M. Alam, M.D. Hossain, B.K. Pramanik, L.N. Nguyen, L.D. Nghiem, M.F. Ahmed, J.L. Zhou, M.I. H. Mondal, M.A. Hossain, M.A.H. Johir, M.B. Ahmed, J.A. Sithi, M. Zargar, M.A. Moni, Metals in e-waste: occurrence, fate, impacts and remediation technologies, Process Saf. Environ. Prot. 162 (2022) 230–252, https://doi.org/10.1016/j.psep.2022.04.011.

[8] K. Staszak, M. Regel-Rosocka, Removing heavy metals: cutting-edge strategies and advancements in biosorption technology, Materials 17 (5) (2024) 1155, https://doi.org/10.3390/ma17051155.

[9] M.O. Idris, A.A. Yaqoob, M.N.M. Ibrahim, A. Ahmad, M.B. Alshammari, Introduction of adsorption techniques for heavy metals remediation, in: A. Ahmad, R. Kumar, M. Jawaid (Eds.), Emerging Techniques for Treatment of Toxic Metals from Wastewater, Elsevier, 2023, pp. 1–18, https://doi.org/10.1016/B978-0-12-822880-7.00024-8.

[10] Y. Fei, Y.H. Hu, Design, synthesis, and performance of adsorbents for heavy metal removal from wastewater: a review, J. Mater. Chem. A 10 (3) (2022) 1047–1085, https://doi.org/10.1039/D1TA06612A.

[11] K.H.H. Aziz, F.S. Mustafa, K.M. Omer, S. Hama, R.F. Hamarawf, K.O. Rahman, Heavy metal pollution in the aquatic environment: efficient and low-cost removal approaches to eliminate their toxicity: a review, RSC Adv. 13 (26) (2023) 17595–17610, https://doi.org/10.1039/D3RA00723E.

[12] M. Date, D. Jaspal, Dyes and heavy metals: removal, recovery and wastewater reuse—a review, Sustain. Water Resour. Manag. 10 (2) (2024) 90, https://doi.org/10.1007/s40899-024-01073-8.

[13] M.H. Rahman, M.A. Islam, M.M. Islam, M.A. Rahman, S.N. Alam, Biodegradable composite adsorbent of modified cellulose and chitosan to remove heavy metal ions from aqueous solution, Curr. Res. Green Sustain. Chem. 4 (2021) 100119, https://doi.org/10.1016/j.crgsc.2021.100119.

[14] A. Singh, S.S. Shah, C. Sharma, V. Gupta, A.K. Sundramoorthy, P. Kumar, S. Arya, An approach towards different techniques for detection of heavy metal ions and their removal from waste water, J. Environ. Chem. Eng. 12 (3) (2024) 113032, https://doi.org/10.1016/j.jece.2024.113032.

[15] M.A. Rahman, D. Lamb, M.M. Rahman, M.M. Bahar, P. Sanderson, Adsorption–desorption behavior of arsenate using single and binary iron-modified biochars: thermodynamics and redox transformation, ACS Omega 7 (1) (2022) 101–117, https://doi.org/10.1021/acsomega.1c04129.

[16] B. Wang, J. Lan, C. Bo, B. Gong, J. Ou, Adsorption of heavy metal onto biomass-derived activated carbon, RSC Adv. 13 (7) (2023) 4275–4302, https://doi.org/10.1039/D2RA07911A.

[17] Y. Niu, W. Hu, M. Guo, Y. Wang, J. Jia, Z. Hu, Preparation of cotton-based fibrous adsorbents for the removal of heavy metal ions, Carbohydr. Polym. 225 (2019) 115218, https://doi.org/10.1016/j.carbpol.2019.115218.

[18] H. Chakhtouna, H. Benzeid, N. Zari, A.E.K. Qaiss, R. Bouhfid, Recent advances in eco-friendly composites derived from lignocellulosic biomass for wastewater treatment, Biomass Convers. Bioref. 14 (11) (2024) 12085–12111, https://doi.org/10.1007/s13399-022-03159-9.

[19] M.I.H. Mondal, M.I. Haque, F. Ahmed, Durable biobased hybrid compounds: potential modifying agents for the development of functional cotton fabrics, Arab. J. Chem. 16 (9) (2023) 105093, https://doi.org/10.1016/j.arabjc.2023.105093.

[20] S. Rattanaphani, M. Chairat, J.B. Bremner, V. Rattanaphani, An adsorption and thermodynamic study of lac dyeing on cotton pretreated with chitosan, Dyes Pigments 72 (1) (2007) 88–96, https://doi.org/10.1016/j.dyepig.2005.08.002.

[21] M.I.H. Mondal, M.K. Islam, F. Ahmed, Effect of silane coupling agents on cotton fibre finishing, J. Nat. Fibers 19 (13) (2022) 5451–5464, https://doi.org/10.1080/15440478.2021.1875382.

[22] M.H. Rahman, A. Hossen, M.I.H. Mondal, A multifunctional aspect of surface modification of cotton fabric with green synthesized titanium dioxide/iron nanocomposite using Psidium guajava leave extract, J. Text. Inst. (2024) 1–11, https://doi.org/10.1080/00405000.2024.2398355.

[23] M. Akram, B. Khan, M. Imran, I. Ahmad, H. Ajaz, M. Tahir, F. Rabbani, I. Kaleem, M.N. Akhtar, N. Ahmad, N.S. Shah, Biosorption of lead by cotton shells powder: characterization and equilibrium modeling study, Int. J. Phytoremediation 21 (2) (2019) 138–144, https://doi.org/10.1080/15226514.2018.1488810.

[24] M.M. Bashar, M.A. Khan, An overview on surface modification of cotton fiber for apparel use, J. Polym. Environ. 21 (2013) 181–190, https://doi.org/10.1007/s10924-012-0476-8.

[25] M.I.H. Mondal, M.M.R. Khan, Characterization and process optimization of indigo dyed cotton denim garments by enzymatic wash, Fash. Text. 1 (2014) 1–12, https://doi.org/10.1186/s40691-014-0019-0.

[26] M. Marchetti, A. Clement, B. Loubinoux, P. Gerardin, Decontamination of synthetic solutions containing heavy metals using chemically modified sawdusts bearing polyacrylic acid chains, J. Wood Sci. 46 (4) (2000) 331–333, https://doi.org/10.1007/BF00766226.

[27] L. Gao, Z. Li, W. Yi, L. Wang, N. Song, W. Zhang, G. Li, S. Wang, N. Li, A. Zhang, Effective Pb^{2+} adsorption by calcium alginate/modified cotton stalk biochar aerogel spheres: with application in actual wastewater, J. Environ. Chem. Eng. 11 (1) (2023) 109074, https://doi.org/10.1016/j.jece.2022.109074.

[28] Y. Guo, L. Wang, J. Sun, Z. Qi, J. Hu, Y. Huang, Y. Chen, J. Wei, X. Wang, J. Kong, H. Zhang, X. Zhang, H. Wang, Macromolecular grafting of carboxyl polymers on the surface of non-woven fabrics and their adsorption behavior on metal cations, J. Colloid Interface Sci. 653 (2024) 707–720, https://doi.org/10.1016/j.jcis.2023.09.056.

[29] R.R. Navarro, K. Sumi, N. Fujii, M. Matsumura, Mercury removal from wastewater using porous cellulose carrier modified with polyethyleneimine, Water Res. 30 (10) (1996) 2488–2494, https://doi.org/10.1016/0043-1354(96)00143-1.

[30] G. Zhang, R. Qu, C. Sun, C. Ji, H. Chen, C. Wang, Y. Niu, Adsorption for metal ions of chitosan coated cotton fiber, J. Appl. Polym. Sci. 110 (4) (2008) 2321–2327, https://doi.org/10.1002/app.27515.

[31] R. Qu, C. Sun, M. Wang, C. Ji, Q. Xu, Y. Zhang, C. Wang, H. Chen, P. Yin, Adsorption of Au (III) from aqueous solution using cotton fiber/chitosan composite adsorbents, Hydrometallurgy 100 (1–2) (2009) 65–71, https://doi.org/10.1016/j.hydromet.2009.10.008.

[32] M.H. Rahman, M. Sofiuzzaman, M.I.H. Mondal, A. Rahman, F. Ahmed, M.M. Islam, M.A. Habib, Recent advancement of PVA/Chitosan-Based composite biofilm for food packaging, Biomed. J. Sci. Tech. Res. 46 (1) (2022) 36982–36986, https://doi.org/10.26717/BJSTR.2022.46.007286.

[33] J. Saha, M.I.H. Mondal, Antimicrobial, UV resistant and thermal comfort properties of chitosan- and aloe vera-modified cotton woven fabric, J. Polym. Environ. 27 (2019) 405–420, https://doi.org/10.1007/s10924-018-1354-9.

[34] M.E.A. Ali, M.M.S. Aboelfadl, A.M. Selim, H.F. Khalil, G.M. Elkady, Chitosan nanoparticles extracted from shrimp shells, application for removal of Fe(II) and Mn(II) from aqueous phases, Separ. Sci. Technol. 53 (2018) 2870–2881, https://doi.org/10.1080/01496395.2018.1489845.

[35] M.A. Abdelhakeem, M.M. Ramadan, F.S. Basaad, Removing of heavymetals from water by chitosan nanoparticles, J. Adv. Chem. 11 (7) (2016) 3765–3771.

[36] C. Liu, B. Wang, Y. Deng, B. Cui, J. Wang, W. Chen, S.Y. He, Performance of a new magnetic chitosan nanoparticle to remove arsenic and its separation from water, J. Nanomater. 2015 (2015) 191829, https://doi.org/10.1155/2015/191829, 9.

[37] S.M. Seyedi, B. Anvaripour, M. Motavassel, N. Jadidi, Comparative Cadmium Adsorption from water by nanochitosan and chitosan, Int. J. Eng. Innov. Technol. (IJEIT) 2 (9) (2013) 145–148.

[38] A. Ma'ruf, S.J.N.E. Hartati, Production and characterization of nano-chitosan from blood clamshell (anadara granosa) by ionic gelation, Nat. Environ. Pollut. Technol. 21 (4) (2022) 1761–1766, https://doi.org/10.46488/NEPT.2022.v21i04.031.

[39] M. Agarwal, M.K. Agarwal, N. Shrivastav, S. Pandey, R. Das, P. Gaur, Preparation of chitosan nanoparticles and their in-vitro characterization, Int. J. Life Sci. Sci. Res. 4 (2) (2018) 1713–1720, https://doi.org/10.21276/ijlssr.2018.4.2.17.

[40] M.S. Salman, M.C. Sheikh, M.M. Hasan, M.N. Hasan, K.T. Kubra, A.I. Rehan, M.E. Awual, A.I. Rasee, R.M. Waliullah, M.S. Hasan, M.A. Khaleque, A.K. D. Alsukaibi, H.M. Alshammari, M.R. Awual, Chitosan-coated cotton fiber composite for efficient toxic dye encapsulation from aqueous media, Appl. Surf. Sci. 622 (2023) 157008, https://doi.org/10.1016/j.apsusc.2023.157008.

[41] A.G. Paulino, A.J. da Cunha, R.V. da Silva Alfaya, A.A. da Silva Alfaya, Chemically modified natural cotton fiber: a low-cost biosorbent for the removal of the Cu (II), Zn (II), Cd (II), and Pb (II) from natural water, Desalination Water Treat. 52 (22–24) (2014) 4223–4233, https://doi.org/10.1080/19443994.2013.804451.

[42] S.I. Rojas, D.C. Duarte, S.D. Mosquera, F. Salcedo, J.P. Hinestroza, J. Husserl, Enhanced biosorption of Cr(VI) using cotton fibers coated with chitosan-role of ester bonds, Water Sci. Technol. 78 (3) (2018) 476–486, https://doi.org/10.2166/wst.2018.284.

[43] E. Rochima, S.Y. Azhary, R.I. Pratama, C. Panatarani, I.M. Joni, Preparation and characterization of nanochitosan from crab shell waste by beads-milling method, in: IOP Conference Series: Mater. Sci. Eng., vol. 193, 2017 012043, https://doi.org/10.1088/1757-899X/193/1/012043, 1.

[44] N.A. Khalil, A.S.A. Rahman, A.M.A. Huraira, S.N.D.F. Janurin, A.N.S. Fizal, N. Ahmad, M. Zulkifli, M.S. Hossain, A.N.A. Yahaya, Magnetic chitosan hydrogel beads as adsorbent for copper removal from aqueous solution, Mater. Today Proc. 74 (2023) 499–503, https://doi.org/10.1016/j.matpr.2022.12.018.

[45] A.M. Khalid, M.S. Hossain, N.A. Khalil, M. Zulkifli, M.A. Arafath, M.S. Shaharun, R. Ayub, A.N.A. Yahaya, N. Ismail, Adsorptive elimination of heavy metals from aqueous solution using magnetic chitosan/cellulose-Fe(III) composite as a bio-sorbent, Nanomaterials 13 (2023) 1595, https://doi.org/10.3390/nano13101595.

[46] Q.S. Liu, T. Zheng, P. Wang, J.P. Jiang, N. Li, Adsorption isotherm, kinetic and mechanism studies of some substituted phenols on activated carbon fibers, Chem. Eng. J. (Amsterdam, Neth.) 157 (2–3) (2010) 348–356, https://doi.org/10.1016/j.cej.2009.11.013.

[47] A. Maleki, B. Hayati, F. Najafi, F. Gharibi, S.W. Joo, Heavy metal adsorption from industrial wastewater by PAMAM/TiO_2 nanohybrid: preparation, characterization and adsorption studies, J. Mol. Liq. 224 (2016) 95–104, https://doi.org/10.1016/j.molliq.2016.09.060.

[48] S.V. Mohan, J. Karthikeyan, Removal of lignin and tannin colour from aqueous solution by adsorption onto activated charcoal, Environ. Pollut. 97 (1–2) (1997) 183–187, https://doi.org/10.1016/S0269-7491(97)00025-0.

[49] M. Foroughi-Dahr, H. Abolghasemi, N. Esmaili, A. Shojamoradi, H. Fatoorehchi, Adsorption characteristics of Congo red from aqueous solution onto tea waste, Chem. Eng. Commun. 202 (2) (2015) 181–193, https://doi.org/10.1080/00986445.2013.836633.

[50] S.S. Gupta, K.G. Bhattacharyya, Kinetics of adsorption of metal ions on inorganic materials: a review, Adv. Colloid Interface Sci. 162 (1–2) (2011) 39–58, https://doi.org/10.1016/j.cis.2010.12.004.

[51] M.M. Roy, M.T. Hossain, M.Z. Hasan, K. Islam, M. Rokonuzzaman, M.A. Islam, S. Khandakar, M.M. Bashar, Adsorption, kinetics and thermodynamics of reactive dyes on chitosan treated cotton fabric, Text Leather Rev 6 (2023) 211–232, https://doi.org/10.31881/TLR.2023.030.

[52] P. Saha, S. Chowdhury, Insight into adsorption thermodynamics, Thermodynamics 16 (2011) 349–364, https://doi.org/10.5772/13474.

[53] X. Zhou, X. Zhou, The unit problem in the thermodynamic calculation of adsorption using the Langmuir equation, Chem. Eng. Commun. 201 (11) (2014) 1459–1467, https://doi.org/10.1080/00986445.2013.818541.

[54] A. Hebeish, K. Elnagar, M.H. Helal, M.S. Ragab, M.F. Shaaban, UV/O_3 preirradiated cotton fabric-containing chitosan for effective removal of heavy metals, Mater. Sci. Appl. 5 (10) (2014) 698, https://doi.org/10.4236/msa.2014.510071.

[55] D. Alonso, M. Gimeno, R. Olayo, H. Vázquez-Torres, J.D. Sepúlveda-Sánchez, K. Shirai, Cross-linking chitosan into UV-irradiated cellulose fibers for the preparation of antimicrobial-finishedtextiles, Carbohydr. Polym. 77 (3) (2009) 536–543, https://doi.org/10.1016/j.carbpol.2009.01.027.

[56] Y.H. Park, S. Kim, J.S. Choi, J. Chung, J.S. Choi, Y.E. Choi, Chitosan-modified cotton fiber: an efficient and reusable adsorbent in removal of harmful cyanobacteria, Microcystis aeruginosa from aqueous phases, Chemosphere 349 (2024) 140679, https://doi.org/10.1016/j.chemosphere.2023.140679.

[57] D.R. Bhumkar, V.B. Pokharkar, Studies on effect of pH on cross-linking of chitosan with sodium tripolyphosphate: a technical note, AAPS PharmSciTech 7 (2) (2006) E1–E6, https://doi.org/10.1208/pt070250. Article no. 50.

[58] S.D. Sarkar, B.L. Farrugia, T.R. Dargaville, S. Dhara, Physico-chemical/biological properties of tripolyphosphate cross-linked chitosan based nanofibers, Mater. Sci. Eng. C 33 (3) (2013) 1446–1454, https://doi.org/10.1016/j.msec.2012.12.066.

[59] R.N. Wijesena, N.D. Tissera, K.N. de Silva, Coloration of cotton fibers using nano chitosan, Carbohydr. Polym. 134 (2015) 182–189, https://doi.org/10.1016/j.carbpol.2015.07.088.

[60] R. Subramaniam, M.P. Mani, S.K. Jaganathan, Fabrication and testing of electrospun polyurethane blended with chitosan nanoparticles for vascular graft applications, Cardiovasc. Eng. Technol. 9 (2018) 503–513, https://doi.org/10.1007/s13239-018-0357-y.

[61] G. Cardenas, S.P. Miranda, FTIR and TGA studies of chitosan composite films, J. Chil. Chem. Soc. 49 (4) (2004) 291–295.

[62] X.-L. Li, X.-H. Shi, M.-J. Chen, Q.-Y. Liu, Y.-M. Li, Z. Li, Y.-Z. Huan, D.-Y. Wang, Biomass-based coating from chitosan for cotton fabric with excellent flame retardancy and improved durability, Cellulose 29 (2022) 5289–5303, https://doi.org/10.1007/s10570-022-04566-x.

[63] M.I.H. Mondal, Mechanism of structure formation of microbial cellulose during nascent stage, Cellulose 20 (2013) 1073–1088, https://doi.org/10.1007/s10570-013-9880-z.

[64] N. Ayawei, A.N. Ebelegi, D. Wankasi, Modelling and interpretation of adsorption isotherms, J. Chem. 2017 (1) (2017) 3039817, https://doi.org/10.1155/2017/3039817.

[65] A.A. Al-Kahtani, Effective removal of heavy metals from aqueous solution using CS/OMMT nanocomposite synthesized by gamma irradiation, J. King Saud Univ. Sci. 36 (3) (2024) 103085, https://doi.org/10.1016/j.jksus.2023.103085.

[66] R. Qu, C. Sun, F. Ma, Y. Zhang, C. Ji, Q. Xu, H. Chen, Removal and recovery of Hg (II) from aqueous solution using chitosan-coated cotton fibers, J. Hazard Mater. 167 (1–3) (2009) 717–727, https://doi.org/10.1016/j.jhazmat.2009.01.043.

[67] S. Jamshidifard, S. Koushkbaghi, S. Hosseini, S. Rezaei, A. Karamipour, A. Jafari rad, M. Irani, Incorporation of UiO-66-NH_2 MOF into the PAN/chitosan nanofibers for adsorption and membrane filtration of Pb(II), Cd(II) and Cr(VI) ions from aqueous solutions, J. Hazard Mater. 368 (2019) 10–20, https://doi.org/10.1016/j.jhazmat.2019.01.024.

[68] R.E.K. Billah, M.A. Islam, M.K. Nazal, L. Bahsis, A. Soufiane, Y. Abdellaoui, M. Achak, A novel glutaraldehyde cross-linked chitosan@ acid-activated bentonite composite for effective Pb (II) and Cr (VI) adsorption: experimental and theoretical studies, Sep. Purif. Technol. 334 (2024) 126094, https://doi.org/10.1016/j.seppur.2023.126094.

[69] P. Liang, S. Liu, M. Li, W. Xiong, X. Yao, T. Xing, K. Tian, Effective adsorption and removal of Cr (VI) from wastewater using magnetic composites prepared by synergistic effect of polypyrrole and covalent organic frameworks, Sep. Purif. Technol. 336 (2024) 126222, https://doi.org/10.1016/j.seppur.2023.126222.

[70] H. Chen, R. Xiao, D. Huang, R. Deng, R. Li, Y. Chen, W. Zhou, Three kinds of apatite adsorbents prepared by co-precipitation for Pb (II) and Cd (II) removal from wastewater: performance, competitive effects and mechanisms, J. Mol. Liq. 400 (2024) 124478, https://doi.org/10.1016/j.molliq.2024.124478.
[71] A.D. Pournara, A. Margariti, G.D. Tarlas, A. Kourtelaris, V. Petkov, C. Kokkinos, A. Economau, G.S. Papaefstathiou, M.J. Manos, A Ca^{2+} MOF combining highly efficient sorption and capability for voltammetric determination of heavy metal ions in aqueous media, J. Mater. Chem. A 7 (25) (2019) 15432–15443, https://doi.org/10.1039/C9TA03337H.
[72] L. Huang, M. Li, H. Lin, Q. Feng, Q. Hu, Z. Chen, J. Lv, J. Lin, L. Li, X. Wu, A novel magnetic and amino grafted chitosan-based composite for efficient adsorption and reduction of Cr(VI): performance and removal mechanism, J. Polym. Environ. 32 (2024) 6375–6389, https://doi.org/10.1007/s10924-024-03390-7.
[73] S. Hokkanen, E. Repo, T. Suopajärvi, H. Liimatainen, J. Niinimaa, M. Sillanpää, Adsorption of Ni (II), Cu (II) and Cd (II) from aqueous solutions by amino modified nanostructured microfibrillated cellulose, Cellulose 21 (2014) 1471–1487, https://doi.org/10.1007/s10570-014-0240-4.
[74] C. Lin, S. Qiao, W. Luo, Y. Liu, D. Liu, X. Li, M. Liu, Thermodynamics, kinetics, and regeneration studies for adsorption of Cr (VI) from aqueous solutions using modified cellulose as adsorbent, Bioresources 9 (4) (2014) 6998–7017, https://doi.org/10.15376/biores.9.4.6998-7017.
[75] X. Yu, S. Tong, M. Ge, L. Wu, J. Zuo, C. Cao, W. Song, Adsorption of heavy metal ions from aqueous solution by carboxylated cellulose nanocrystals, J. Environ. Sci. 25 (5) (2013) 933–943, https://doi.org/10.1016/S1001-0742(12)60145-4.
[76] L. Zhang, S. Tang, F. He, Y. Liu, W. Mao, Y. Guan, Highly efficient and selective capture of heavy metals by poly(acrylic acid) grafted chitosan and biochar composite for wastewater treatment, Chem. Eng. J. (Amsterdam, Neth.) 378 (2019) 122215, https://doi.org/10.1016/j.cej.2019.122215.
[77] S.S. Li, X.L. Wang, Q.D. An, Z.Y. Xiao, S.R. Zhai, L. Cui, Z.C. Li, Upon designing carboxyl methylcellulose and chitosan-derived nanostructured sorbents for efficient removal of Cd (II) and Cr (VI) from water, Int. J. Biol. Macromol. 143 (2020) 640–650, https://doi.org/10.1016/j.ijbiomac.2019.12.053.
[78] R. Yu, Y. Shi, D. Yang, Y. Liu, J. Qu, Z.Z. Yu, Graphene Oxide/Chitosan aerogel microspheres with honeycomb-cobweb and radially oriented microchannel structures for broad-spectrum and rapid adsorption of water contaminants, ACS Appl. Mater. Interfaces 9 (26) (2017) 21809–21819, https://doi.org/10.1021/acsami.7b04655.
[79] K. Rathinam, S.P. Singh, C.J. Arnusch, R. Kasher, An environmentally- friendly chitosan-lysozyme biocomposite for the effective removal of dyes and heavy metals from aqueous solutions, Carbohydr. Polym. 199 (2018) 506–515, https://doi.org/10.1016/j.carbpol.2018.07.055.
[80] J. Ma, Y. Liu, O. Ali, Y. Wei, S. Zhang, Y. Zhang, T. Cai, C. Liu, S. Luo, Fast adsorption of heavy metal ions by waste cotton fabrics based double network hydrogel and influencing factors insight, J. Hazard Mater. 344 (2018) 1034–1042, https://doi.org/10.1016/j.jhazmat.2017.11.041.
[81] D.M. Guo, Q.D. An, Z.Y. Xiao, S.R. Zhai, D.J. Yang, Efficient removal of Pb(II), Cr(VI) and organic dyes by polydopamine modified chitosan aerogels, Carbohydr. Polym. 202 (Ii) (2018) 306–314, https://doi.org/10.1016/j.carbpol.2018.08.140.
[82] J. Dong, L. Shen, S. Shan, W. Liu, Z. Qi, C. Liu, X. Gao, Optimizing magnetic functionalization conditions for efficient preparation of magnetic biochar and adsorption of Pb (II) from aqueous solution, Sci. Total Environ. 806 (2022) 151442, https://doi.org/10.1016/j.scitotenv.2021.151442.
[83] A. Razzaz, S. Ghorban, L. Hosayni, M. Irani, M. Aliabadi, Chitosan nanofibers functionalized by TiO2 nanoparticles for the removal of heavy metal ions, J. Taiwan Inst. Chem. Eng. 58 (2016) 333–343, https://doi.org/10.1016/j.jtice.2015.06.003.
[84] I. Ijaz, A. Bukhari, A. Nazir, E. Gilani, H. Zain, S. Hussain, H. Ahmad, Enhanced selective adsorption capacity of lead (II) from complex wastewater by aminopropyltriethoxysilane-functionalized biochar grafted on the MXene based on anion-synergism, Mater. Chem. Phys. 314 (2024) 128929, https://doi.org/10.1016/j.matchemphys.2024.128929.
[85] Y.P. Kunar, P. King, V.S.R.K. Prasad, Adsorption of zinc from aqueous solution using marine green algae-Ulva Fasciata sp, J. Chem. Eng. 129 (2007) 161–166, https://doi.org/10.1016/j.cej.2006.10.023.
[86] Y. Xiao, G. Shen, W. Zheng, J. Fu, F. Fu, X. Hu, Z. Jin, X. Liu, Remarkable durability of the antibacterial function achieved via a coordination effect of Cu(II) ion and chitosan grafted on cotton fibers, Cellulose 29 (2022) 1003–1015, https://doi.org/10.1007/s10570-021-04281-z.
[87] E.D. Revellame, D.L. Fortela, W. Sharp, R. Hernandez, M.E. Zappi, Adsorption kinetic modeling using pseudo-first order and pseudo-second order rate laws: a review, Clean. Eng. Technol. 1 (2020) 100032, https://doi.org/10.1016/j.clet.2020.100032.
[88] F.A. Razmi, N. Ngadi, S. Wong, I.M. Inuwa, L.A. Opotu, Kinetics, thermodynamics, isotherm and regeneration analysis of chitosan modified pandan adsorbent, J. Clean. Prod. 231 (2019) 98–109, https://doi.org/10.1016/j.jclepro.2019.05.228.